

# A REDUCED MODEL FOR NEPHRON FLOW DYNAMICS MEDIATED BY TUBULOGLOMERULAR FEEDBACK

E. BRUCE PITMAN\*, ROMAN M. ZARITSKI†, LEON C. MOORE‡, AND  
H. E. LAYTON§

**Abstract.** Previously we developed a “minimal” mathematical model of the tubuloglomerular feedback (TGF) system in a short-looped nephron of the mammalian kidney. In that model, a hyperbolic partial differential equation (PDE) represented the advection and transepithelial transport of chloride in the thick ascending limb (TAL). The feedback response was represented by an empirical relationship that determined the glomerular filtration rate as a function of time-delayed TAL luminal chloride concentration alongside the macula densa. This PDE model system with feedback and a time delay presents analytical and computational challenges. In this report, we derive a reduced model that is based on the minimal model. The reduced model, which is formulated as an integral equation in time, is easier to study than the PDE model. As in the case of the minimal model, analysis of the reduced model suggests that sustained oscillations in nephron fluid flow arise from a Hopf bifurcation, with delay time and system gain as bifurcation parameters. Both analysis and numerical calculations indicate that the principal bifurcation locus predicted by the reduced model coincides with the analogous locus obtained from the minimal model. Near the principal bifurcation locus, numerical solutions of the two models nearly coincide. For bifurcation parameters that differ sufficiently from the principal bifurcation locus, the numerical solutions to the two models differ somewhat. The reduced TGF model has the potential to facilitate simulation and analysis of interactions among TGF systems in multiple nephrons.

**Key words.** Mathematical model, functional differential equations, Hopf bifurcation, renal autoregulation, kidney

**AMS(MOS) subject classifications.** Primary 35L99, 92C35; secondary 34K18.

**1. Introduction.** Tubuloglomerular feedback (TGF) is an important controller of kidney function. A distinct TGF system operates in each of the nephrons, which are the primary functional units of the kidney. TGF regulates the flow of fluid leaving the proximal parts of a nephron (the proximal tubule and Henle’s loop) by monitoring the NaCl concentration of the tubular fluid as it passes the macula densa (MD), a plaque of specialized cells in the wall of the thick ascending limb (TAL) of Henle’s loop (see Fig. 1, below). When the MD is stimulated by an increase in the NaCl concentration of the tubular fluid (an increase that normally occurs when TAL fluid flow increases) a signal is directed to the afferent arteriole (AA) that supplies blood to that same nephron. In response, the AA

---

\*Department of Mathematics, State University of New York, Buffalo, NY 14214-3093.

† Department of Mathematics, State University of New York, Buffalo, NY 14214-3093. Present address: Department of Computer Science, Montclair State University, Upper Montclair, NJ 07043.

‡Department of Physiology and Biophysics, State University of New York, Stony Brook, New York 11794-8661.

§Department of Mathematics, Duke University, Durham, North Carolina 27708-0320.

constricts, which reduces the blood flow to, and the hydrostatic pressure within, the glomerular capillaries, resulting in a reduced rate of filtration into the nephron. By this means, TGF balances the load of fluid presented to the nephron with the capacity of tubular epithelial cells to absorb and process the filtered fluid. TGF also participates in the stabilization of renal blood flow and glomerular filtration rate in response to fluctuations in systemic arterial blood pressure, a phenomenon called renal autoregulation [21].

Fluid flow in the nephrons of normotensive rats either approximates a time-independent steady state or exhibits sustained limit-cycle oscillations (LCO) with frequency of about 25-50 mHz [9, 11]. Fluid flow in the nephrons of hypertensive rats often exhibits irregular oscillations that are suggestive of deterministic chaos [22]. Experiments have established that the flow oscillations, whether LCO or irregular oscillations, involve the TGF system [11].

Several mathematical models have been formulated to elucidate the origins of these flow oscillations [1, 8, 10, 13, 18]. In previous work, we formulated a “minimal” dynamic model of fluid flow and solute advection in a nephron [13]. In that model, a hyperbolic partial differential equation (PDE) represents the advection and transepithelial transport of chloride in the TAL. Feedback is represented by an empirical relationship that determines glomerular filtration, and hence TAL flow speed, as a function of the intratubular chloride concentration sensed by the MD at an earlier time. This results in a time-delay PDE. Analysis and numerical computations show that model behavior depends critically on at least two parameters, the delay  $\tau$  at the MD and the feedback loop gain  $\gamma$ ; indeed, the analysis suggests that a Hopf bifurcation occurs along a locus in the  $\tau$ - $\gamma$  parameter space [13]. The bifurcation locus marks the loss of stability of time-independent steady-state model solutions and the appearance of stable LCO. The range of physiological parameters measured in the kidneys of normotensive rats is approximately bisected by the bifurcation locus, which may help explain why some nephrons exhibit LCO while others do not. The minimal model is summarized below in Section 2.

The minimal TGF model has been robust in its agreement with experimental data [13, 14, 15, 16, 17]. However, its use of a PDE to describe transport in the TAL limits the possibilities for analysis and presents a significant computational burden in simulation studies involving the interactions of TGF systems in multiple nephrons, a case of considerable physiological importance. Studies in rats show that 50–60% of the superficial nephrons occur in pairs (and some triples), where the afferent arterioles feeding these nephrons branch from a common location, either on a cortical radial artery (CRA) or on a short connecting artery that branches from a CRA [3]. Such nephron pairs (or triplets) are said to have a close vascular connection.

Renal micropuncture experiments have shown that nephron pairs with

close vascular connection, or which branch from discrete sites on the same CRA, usually exhibit synchronous flow oscillations, whereas flow oscillations tend to be uncoordinated in nephron pairs perfused by different CRAs [7]. Yip et al. confirmed that a close vascular coupling of nephron pairs on the CRA is strongly correlated with synchronous oscillations [23]. They also found evidence suggesting that the magnitude of nephron-nephron interaction is greater in hypertensive rats, relative to normotensive animals. Chen et al. verified these findings and found that the strength of the nephron-nephron interaction varies inversely with the length of the vascular structures interposed between the nephrons [5]. Together, these experimental studies provide strong evidence for interaction, or coupling, of nephrons via vascular pathways. The mechanism of vascular coupling most likely involves electrotonic conduction of signals through the gap junctions that connect the smooth muscle and endothelial cells in the AA and CRA [5].

In Ref. [19], we formulated a model for two coupled nephrons as a generalization of our minimal single-nephron model. The two-nephron model contains two hyperbolic PDEs that are coupled via the tubular flows that are determined by the feedback responses. Our investigation shows that an analytical bifurcation analysis is possible for special cases. The results suggest that, by displacing the bifurcation locus, close vascular coupling facilitates the emergence of oscillations, relative to uncoupled nephrons [19]. Numerical simulations further suggest that dynamic behaviors more complex than LCO can be elicited in this model of two coupled nephrons [24]. However, analysis of our TGF models involves the study of bifurcations of a hyperbolic PDE with a time delay—a difficult, non-standard problem in applied mathematics.

In Section 3, we derive from our minimal model a new, “reduced” model of TGF. The reduced model is an integral equation that arises from a linearization of the characteristic form of the original PDE model. Analysis of this reduced model yields the same principal bifurcation locus as the PDE model, and numerical calculations show that the dynamic behaviors of the two models are similar. The reduced model eliminates some of the computational difficulties of the minimal model and thus may be well-suited for studies of inter-nephron interaction.

In Section 4, we derive a functional<sup>1</sup> ordinary differential equation (ODE) that is equivalent to our minimal model, provided that the TAL is assumed to be impermeable to NaCl. This formulation of the minimal model, which has a state-dependent time delay, is helpful for explaining the difficulties inherent in solving the minimal model, relative to the reduced model.

---

<sup>1</sup>In this context, “functional” means that the differential equation contains a delay in the time variable [6]; such a differential equation is also called a delay differential equation or a differential-difference equation [2].

**2. The Minimal Model.** In this section, we summarize the minimal model as originally developed in Ref. [13].

**2.1. Model formulation.** The model represents TGF in a short-looped nephron like that found in the rat. Such nephrons have a loop of Henle that reaches nearly to the boundary of the inner and outer medulla (see Fig. 1). The model is formulated as a system of two coupled equations:

$$(2.1) \quad \frac{\partial}{\partial t} C(x, t) = -F(C(1, t - \tau)) \frac{\partial}{\partial x} C(x, t) - \frac{V_{max} C(x, t)}{K_M + C(x, t)} - P(C(x, t) - C_e(x))$$

and

$$(2.2) \quad F(C(1, t - \tau)) = 1 + K_1 \tanh(K_2(C_{op} - C(1, t - \tau))).$$

Both equations are expressed in nondimensional form (see *Normalization of equations*, below). The space variable  $x$  is oriented so that it extends from the entrance of the TAL ( $x = 0$ ), through the outer medulla, and into the cortex to the MD ( $x = 1$ ).

Equation 2.1, which is based on mass conservation of chloride in a rigid tube, is a PDE for the chloride concentration  $C(x, t)$ , at position  $x$  and time  $t$ , in the intratubular fluid of the TAL. At  $x = 0$ , we assume that  $C(0, t) = 1$ , meaning that fluid entering the TAL has constant chloride concentration. The rate of change of that concentration for  $x \in (0, 1]$  depends on processes represented by the three right-hand terms in Eq. 2.1. The first term is axial chloride advection at intratubular flow speed  $F$ . The second is transepithelial efflux of chloride driven by active metabolic pumps situated in the tubular walls; that efflux is approximated by Michaelis-Menten kinetics, with maximum transport rate  $V_{max}$  and Michaelis constant  $K_M$ . The third term is transepithelial chloride backleak, which depends on a specified fixed extratubular chloride concentration profile  $C_e(x)$  and on chloride permeability  $P$ .

Equation 2.2, which represents the feedback response, gives the TAL intratubular fluid speed as a function of  $C(1, \cdot)$ , the intratubular TAL chloride concentration alongside the MD. This equation, which was obtained empirically by physiologists, is well-established by steady-state experiments [20]. The constant  $C_{op}$  is the steady-state chloride concentration obtained at the MD when  $F \equiv 1$ . The positive constants  $K_1$  and  $K_2$  describe, respectively, the range of the feedback response and its sensitivity to deviations from the steady state.

Dynamic experiments [4] show that a change in MD concentration does not significantly affect AA muscle tension until after a positive delay time  $\tau$ . Thus the flow in Eq. 2.1 depends on the MD concentration at the previous time  $t - \tau$ , i.e., on  $C(1, t - \tau)$ . At time  $t = 0$ , the initial TAL

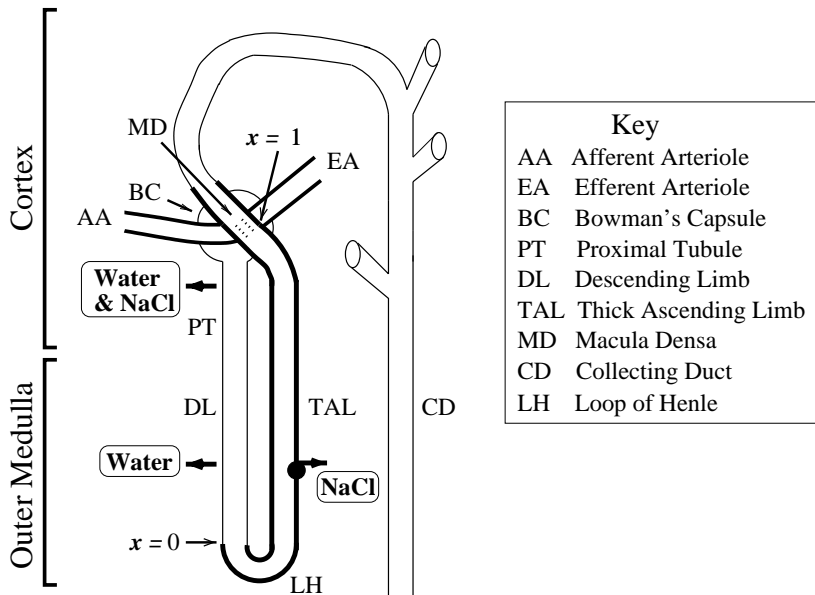


FIG. 1. Schematic drawing of a short-looped nephron. Relationship to cortex and outer medulla is indicated at left. Important structures are labeled according to Key at right. The glomerulus is contained within Bowman's capsule (BC). The macula densa (MD), contrary to the appearance in this drawing, is on the back side of the thick ascending limb (TAL) and adjacent to the region where the glomerulus, afferent arteriole (AA), and efferent arteriole (EA) come together. Water and salt are absorbed from the proximal tubule (PT) and returned to the blood by means of the peritubular capillaries; water is absorbed from the water-permeable descending limb (DL), and NaCl is actively transported from the essentially water-impermeable thick ascending limb (TAL).

concentration profile ( $C(x, 0)$  for  $x \in (0, 1]$ ) and a concentration history at the MD ( $C(1, t)$  for  $t \in [-\tau, 0)$ ) must be specified.

In this study, which aims at analytical simplification, we will assume that solute backleak, which is perhaps the most important second-order transepithelial transport effect, is zero. Thus, we set  $P = 0$  and  $C_e(x)$  need not be specified. For subsequent convenience, we write the remaining transepithelial transport term (the one described by Michaelis Menten kinetics) as a function  $J$  defined by

$$(2.3) \quad J(C) = \frac{V_{max}C}{K_M + C}.$$

A steady-state solution to Eqs. 2.1 and 2.2 may be obtained by setting  $F = 1$  for  $t \in [0, 1 + \tau)$ . The TAL concentration profile will attain a steady state at  $t = 1$ , since the TAL transit time is 1 at flow speed 1; moreover,  $C(1, t) = C_{op}$  in the interval  $t \in [1, 1 + \tau)$ . If the feedback loop is closed at  $t = 1 + \tau$ , then  $F$  will equal 1 for all time such that  $t \geq 1 + \tau$ , and

the steady-state TAL concentration profile will persist, provided that the system remains unperturbed.

Under the assumption of no solute backleak, the steady-state TAL concentration profile of  $C$ , denoted by  $S(x)$ , is given by the solution of the ODE

$$(2.4) \quad S'(x) = -J(S(x)), \quad S(0) = 1,$$

where we have used  $F(S(1)) = F(C_{op}) = 1$  and  $S(0) = C(0, t) = 1$ , and where the prime indicates differentiation with respect to  $x$ .

*Normalization of equations.* The dimensional forms of Eqs. 2.1 and 2.2 are given by

$$(2.5) \quad \frac{\partial}{\partial t} C(x, t) = -\frac{F(C(1, t - \tau))}{\pi r^2} \frac{\partial}{\partial x} C(x, t) - (2/r) \left( \frac{V_{max} C(x, t)}{K_M + C(x, t)} + P (C(x, t) - C_e(x)) \right),$$

and

$$(2.6) \quad F(C(L, t - \tau)) = \alpha \left( Q_{op} + \frac{\Delta Q}{2} \tanh \left( \frac{k}{2} (C_{op} - C(L, t - \tau)) \right) \right),$$

where  $r$  is the tubular radius,  $\alpha$  is the (dimensionless) fraction of single nephron glomerular filtration rate (SNGFR) reaching the TAL,  $Q_{op}$  is the steady-state (operating) SNGFR,  $\Delta Q$  is the TGF-mediated range of SNGFR, and  $k$  is the sensitivity of the TGF response [13]. To express these equations in nondimensional form, let  $\tilde{x} = x/L$ ,  $\tilde{t} = t/t_o$ ,  $\tilde{\tau} = \tau/t_o$ ,  $\tilde{r} = r/\sqrt{A_o/\pi}$ ,  $\tilde{C}(\tilde{x}, \tilde{t}) = C(x, t)/C_o$ ,  $\tilde{C}_e(\tilde{x}) = C_e(x)/C_o$ ,  $\tilde{F}(\tilde{C}(1, \tilde{t} - \tilde{\tau})) = F(C(L, t - \tau))/F_o$ ,  $\tilde{V}_{max} = V_{max}/(V_{max})_o$ ,  $\tilde{K}_M = K_M/C_o$ ,  $\tilde{P} = P/P_o$ ,  $K_1 = \Delta Q/2Q_o$ ,  $K_2 = kC_o/2$ , and  $\tilde{C}_{op} = C_{op}/C_o$ , where  $L$  is TAL length, and the quantities subscripted with an “ $o$ ” are conveniently chosen reference values:  $A_o = \pi r^2$ ,  $t_o = A_o L/F_o$ ,  $C_o = C(0, \cdot)$ ,  $F_o = F_{op} = \alpha Q_{op}$ ,  $(V_{max})_o = F_o C_o/(2\pi r L)$ ,  $P_o = F_o/(2\pi r L)$ , and  $Q_o = Q_{op}$ . With these conventions,  $t_o$  is the filling time (and thus the transit time) of the TAL at flow rate  $F_o$ , and  $(V_{max})_o$  is the rate of solute convection into the inlet of the TAL at flow rate  $F_o$ , divided by the area of the sides of the TAL. When Eqs. 2.5 and 2.6 are rewritten in dimensionless terms and the tilde symbols are dropped, Eqs. 2.1 and 2.2 follow directly.

*Model parameters.* The values of model base-case parameters, assuming no chloride backleak, are given in Table 1; the criteria for their selection and supporting references were given in Ref. [13]. The steady-state operating concentration  $C_{op}$  was calculated numerically using the TAL dimensions and transport parameters, with steady flow  $F = 1$  in Eq. 2.1.

Table 1: *Parameter set for no chloride backleak ( $P = 0$ )*

Parameter	Value
$\alpha$	0.200 (dimensionless)
$C_o$	275 mM
$L$	0.500 cm
$Q_{op}$	30.0 nl/min
$\Delta Q$	18.0 nl/min
$r$	10.0 $\mu\text{m}$
$t_o$	15.708 s
$\tau$	3.5 s
$K_M$	140 mM
$V_{max}$	17.3 nmole $\cdot$ cm $^{-2}$ $\cdot$ s $^{-1}$
$C_{op}$	32.12 mM

**2.2. Bifurcation analysis.** Under normal conditions, renal blood flow is subject to disturbances from a number of physiological sources, such as heartbeat, respiration, and other factors that cause fluctuations in blood pressure. Such disturbances will result in deviations from time-independent steady-state intratubular nephron flow. Thus, an important question is, What is the behavior of a nephron subsequent to a transient perturbation of that steady state? In the context of the minimal nephron model, an answer to this question was provided in Ref. [13]: if the system is perturbed, the stable solution depends on the time delay  $\tau$  and on the gain of the feedback loop (the gain will be determined below).<sup>2</sup> In one region of the delay–gain parameter plane, the perturbed solution tends back to the steady-state. In another region, the steady state is no longer stable and the perturbed solution tends to a regular oscillation, i.e., to an LCO. The two regions in the delay–gain parameter space are separated by a curve, and that curve is the locus of a bifurcation where the time-independent steady-state solution loses stability and the steady state is replaced by a stable LCO (see Fig. 2, below).

In this subsection, we summarize the analysis that predicts the bifurcation from a stable time-independent steady-state to a stable LCO. We first combine Eqs. 2.1 and 2.2 into a single equation, which we linearize by assuming a solution of the form

$$(2.7) \quad C(x, t) = S(x) + \epsilon D(x, t),$$

where, recall,  $S(x)$ , the solution of Eq. 2.4, is the steady-state TAL concentration profile, and where  $D$  represents the deviation from that steady state. To obtain the linearization, expand (by means of a Taylor series in

<sup>2</sup>A physiological perturbation can be simulated by a transient augmentation of flow, an augmentation which may be achieved by adding a small quantity to the right-hand side of Eq. 2.2.

$\epsilon$ ) those terms that are nonlinear in  $\epsilon$ , retaining only the terms that are first order in  $\epsilon$ . This yields a PDE for the deviation, given by

$$(2.8) \quad \frac{\partial}{\partial t} D(x, t) = -\frac{\partial}{\partial x} D(x, t) - J'(S(x))D(x, t) - F'(C_{op})S'(x)D(1, t - \tau),$$

where the primes indicate differentiation with respect to the arguments of the functions. (The terms that are order zero in  $\epsilon$  drop out because they are equivalent to the time-independent steady-state ODE for  $S(x)$ , i.e., to Eq. 2.4.) Because  $C(0, t) = S(0) = 1$ , the boundary condition for  $D(x, t)$  is

$$(2.9) \quad D(0, t) = 0.$$

If the deviation arising from a perturbation of the steady-state diminishes in time, i.e., if the deviation tends to zero in the sense that

$$(2.10) \quad \lim_{t \rightarrow \infty} \left( \max_{x \in [0, 1]} |D(x, t)| \right) = 0,$$

then the time-independent steady-state solution  $S(x)$  is the stable solution. On the other hand, if  $D$  does not tend to zero, then  $S$  is an unstable solution and the stable solution has a TAL concentration profile that varies in time.

We assume that the deviation  $D$  can be written as a product of a function  $f(x)$  that depends only on the spatial variable  $x$  and an exponential function  $e^{\lambda t}$  that depends only on the temporal variable  $t$ . Thus we use the method of separation of variables, and we write

$$(2.11) \quad D(x, t) = f(x)e^{\lambda t},$$

where  $f(0) = 0$  to conform to the boundary condition given by Eq. 2.9. Because the parameter  $\lambda$  can have both a real part ( $\text{Re } \lambda$ ) and an imaginary part ( $\text{Im } \lambda$ ),  $e^{\lambda t}$  can both modify the amplitude of  $D$  and allow oscillations in  $D$ .

If  $\text{Re } \lambda < 0$ , then  $D$  tends to zero in the sense of Eq. 2.10, and the steady-state solution  $S(x)$  is the stable TAL concentration profile. However, if  $\text{Re } \lambda > 0$ , then a perturbation of the steady state may lead to an oscillatory solution of Eq. 2.8, and, indeed, to oscillations that grow without bound. However, in the full model, nonlinearities in Eqs. 2.1 and 2.2 (specifically, nonlinearities in the bounded range of  $F$  and in the Michaelis-Menten kinetics) prevent unbounded oscillations.

If one assumes that the form for  $D$  given in Eq. 2.11 is a solution of the linear PDE given by Eq. 2.8, then that PDE imposes a relationship between  $\lambda$  and the parameters arising in the PDE. That relationship is the characteristic equation, which we now derive. If one substitutes the

assumed form for  $D$  into Eq. 2.8 and cancels the common factor of  $e^{\lambda t}$ , the result is a first-order linear ODE for  $f(x)$  given by

$$(2.12) \quad f'(x) = -\left(\lambda + J'(S(x))\right) f(x) + K_1 K_2 S'(x) f(1) e^{-\lambda \tau},$$

where the primes indicate differentiation with respect to the arguments of the functions, and where  $F'(C_{op})$  has been replaced by  $-K_1 K_2$ . The solution to this ODE can be written as

$$(2.13) \quad f(x) = K_1 K_2 f(1) e^{-\lambda \tau} e^{-h(x)} \int_0^x S'(y) e^{h(y)} dy$$

where

$$(2.14) \quad h(x) = \int_0^x \left(\lambda + J'(S(u))\right) du.$$

By differentiating equation Eq. 2.4 with respect to  $x$ , one obtains  $J'(S(x)) = -S''(x)/S'(x)$ , and thus  $h(x) = \lambda x - \ln |S'(x)|$ . Thus, after simplification, Eq. 2.13 can be written as

$$(2.15) \quad f(x) = -K_1 K_2 f(1) e^{-\lambda \tau} S'(x) \left(\frac{e^{-\lambda x} - 1}{\lambda}\right).$$

If one evaluates this equation at  $x = 1$ , cancels  $f(1)$  from both sides, and defines a new, positive parameter  $\gamma$  by

$$(2.16) \quad \gamma = -K_1 K_2 S'(1),$$

then one obtains the characteristic equation for  $\lambda$ ,

$$(2.17) \quad 1 = \gamma e^{-\lambda \tau} \left(\frac{e^{-\lambda} - 1}{\lambda}\right).$$

This equation contains two dimensionless parameters:  $\tau$ , the normalized time delay, and  $\gamma$ , the feedback loop gain. The gain is a measure of the signal amplification by the feedback loop. (An in-depth treatment of gain is given in Ref. [14]; technically speaking,  $-\gamma$  is the gain whereas  $\gamma$  is the gain magnitude, because gain in a negative feedback system is negative.)

The complex-valued parameter  $\lambda$  can be written  $\lambda = \zeta + i\omega$ , where  $\zeta$  and  $\omega$  are real numbers with  $\text{Re } \lambda = \zeta$  and  $\text{Im } \lambda = \omega$ . The sign of  $\zeta$  determines whether the amplitude of the oscillatory solution is decreasing or increasing. To determine a bifurcation locus separating increasing solution amplitudes from decreasing ones, set  $\zeta = 0$  (i.e., let  $\lambda = i\omega$ ). After algebraic transformations, the characteristic equation can then be written as

$$(2.18) \quad \omega/2 = -\gamma \sin(\omega/2) \left(\cos(\omega(\tau + 1/2)) - i \sin(\omega(\tau + 1/2))\right).$$